



## City Research Online

### City, University of London Institutional Repository

---

**Citation:** Wang, Z. & Giaralis, A. (2020). Enhanced serviceability performance in wind-excited tall buildings equipped with optimal tuned mass damper inerter via top-storey softening. In: EUROODYN 2020 Proceedings of the XI International Conference on Structural Dynamics. (pp. 2103-2112). Greece, Athens: Institute of Research and Development for Computational Methods in Engineering Sciences. ISBN 978-618-85072-2-7

This is the published version of the paper.

This version of the publication may differ from the final published version.

---

**Permanent repository link:** <https://openaccess.city.ac.uk/id/eprint/25164/>

**Link to published version:**

**Copyright:** City Research Online aims to make research outputs of City, University of London available to a wider audience. Copyright and Moral Rights remain with the author(s) and/or copyright holders. URLs from City Research Online may be freely distributed and linked to.

**Reuse:** Copies of full items can be used for personal research or study, educational, or not-for-profit purposes without prior permission or charge. Provided that the authors, title and full bibliographic details are credited, a hyperlink and/or URL is given for the original metadata page and the content is not changed in any way.

---

City Research Online:

<http://openaccess.city.ac.uk/>

[publications@city.ac.uk](mailto:publications@city.ac.uk)

---

## ENHANCED SERVICEABILITY PERFORMANCE IN WIND-EXCITED TALL BUILDINGS EQUIPPED WITH OPTIMAL TUNED MASS DAMPER INERTER VIA TOP-STOREY SOFTENING

Zixiao Wang<sup>1</sup>, Agathoklis Giaralis<sup>2\*</sup>

<sup>1</sup> PhD Candidate, Department of Civil Engineering, City University of London  
Northampton Square, London EC1V 0HB, UK  
e-mail: [Zixiao.Wang@city.ac.uk](mailto:Zixiao.Wang@city.ac.uk)

<sup>2</sup> Senior Lecturer, Department of Civil Engineering, City University of London  
Northampton Square, London EC1V 0HB, UK  
e-mail: [agathoklis.giaralis.1@city.ac.uk](mailto:agathoklis.giaralis.1@city.ac.uk)

**Keywords:** Tuned mass damper inerter, optimal passive vibration control, wind-excited tall buildings, vortex shedding, occupants' comfort, floor acceleration.

**Abstract.** A local structural modification, namely top-storey softening, is herein considered in conjunction with optimally tuned top-floor tuned mass damper inerter (TMDI) for improved serviceability performance in mid-to-high rise buildings (host structures). The focus is to reduce floor accelerations on typical core-frame host structures with rectangular footprint due to wind-induced vortex shedding (VS) effects causing occupants' discomfort. This aim is achieved by formulating an optimal TMDI tuning problem in which TMDI inertial and top-storey host structure properties (i.e., attached mass and inertance, and top-storey height) are treated as design variables, to a case-study building aiming to minimize peak floor acceleration in the across-wind direction. The optimal TMDI tuning problem is numerically solved for a wide range of design variables for a 34-storey composite core-frame building subject to stochastic spatially-correlated wind-force field accounting for VS effects. A planar low-order dynamical model capturing faithfully modal properties of the 34-storey building is developed to facilitate computational work and parametric investigation. It is found that top-storey stiffness reduction, herein regulated through storey height, not only relaxes attached TMDI mass/weight requirements, but also reduces TMDI stroke, and inerter force for fixed performance and inertance. It is concluded that by leveraging inertance and top-storey stiffness, the considered solution can efficiently control VS-induced floor acceleration with small additional gravitational (added weight) and horizontal damping forces to the satisfaction of standard code requirements for occupants comfort.

## 1 INTRODUCTION

Passive dynamic vibration absorbers, including tuned mass-dampers (TMDs), have been widely used for mitigating wind-induced vibrations in tall buildings (e.g., [1,2]). A typical linear TMD comprises a mass attached towards the top of the building (host structure) via linear stiffeners and dampers [3]. The TMD is tuned to the first natural frequency of the building aiming to dampen the fundamental lateral mode shape which tends to be mostly excited due to resonance with the frequency of wind-induced forces. Such forces typically develop in the across-wind direction of tall buildings with rectangular foot-print due to vortex shedding (VS) [4] and may induce large floor accelerations causing occupants' discomfort [5] and, consequently, serviceability structural failure. This consideration becomes critical for slender tall buildings and governs their design [6]. Meanwhile, the applicability of passive TMDs for wind-induced vibration suppression is limited by structural and economical considerations. This is because their motion control potential relies on the attached mass (i.e., the larger it is, the more effective the TMD becomes [7]), but constraints apply to the TMD weight that can be safely accommodated at the top floor of slender/tall buildings while TMD up-front cost increases proportionally with its mass [8].

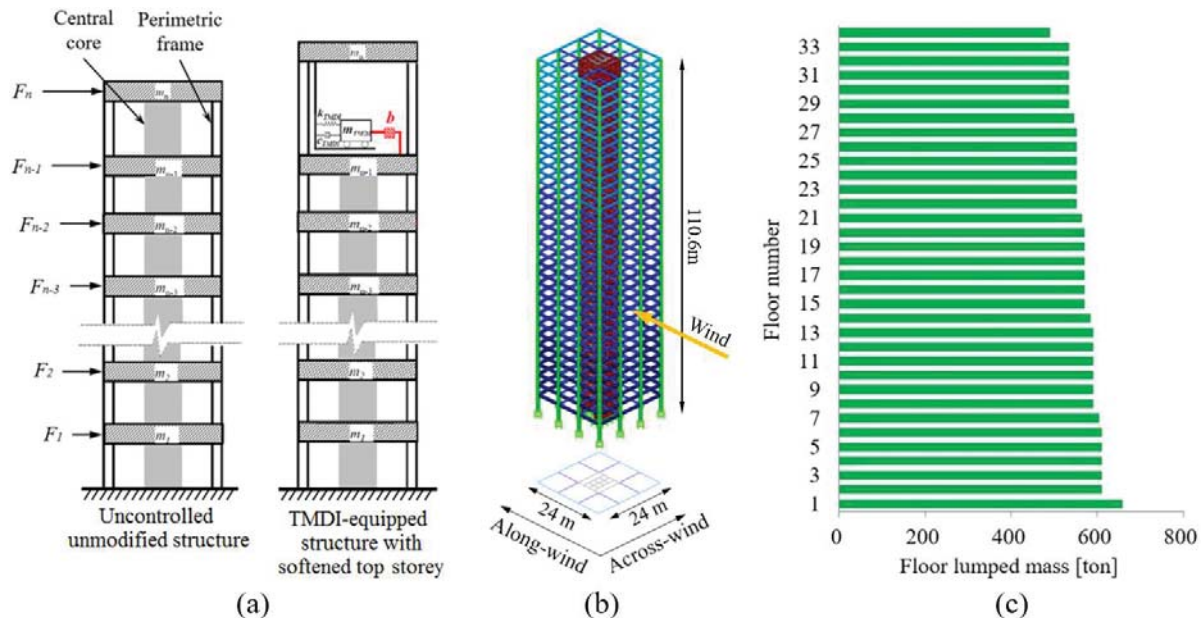


Figure 1 (a) Schematic of a TMDI-equipped planar coupled core-frame building with soft top-storey, (b) case-study 34-storey building, and (c) lumped floor mass distribution.

Recently, it has been shown [9,10] that the incorporation of an inerter to TMD-equipped tall buildings in the so-called tuned mass damper inerter (TMDI) configuration enhances serviceability performance against VS-induced wind forces without increasing the required attached weight, thus overcoming the above TMD limitations. Specifically, the inerter is defined as a linear mechanical element that resists relative acceleration through the inertance constant assuming mass units (kg) [11]. In the TMDI, originally proposed for seismic protection of building structures [12-14], an inerter element is used to link the TMD attached mass to a different floor from the one that the TMD is attached to. It is then found [9,10] that improved floor acceleration mitigation is achieved in tall wind-excited TMDI-equipped buildings by increasing the inertance, which scales-up independently of physical mass in prototyped inerter devices [15,16], and, even more so, by letting the inerter span more than one storey. Nevertheless, for

routine slender mid-to-high-rise buildings with 20-40 storeys, TMDI configuration with inerter spanning more than one floor is not as practical as in the case of tall landmark structures (e.g., [2]) since occupying high-premium space across several upper floors of such structures for accommodating a control device is not cost effective. To this end, this paper explores the potential of a local structural modification, top-storey softening, in conjunction with top-storey TMDI placement as shown in Figure 1(a), to mitigate floor accelerations in the across-wind direction of VS-sensitive buildings with no more than 40 stories. Notably, the above vibration mitigation solution is practically meritorious for such buildings in which standard coupled core-frame systems are used for lateral wind load resistance [17]. This is because: (1) the considered solution does not utilize premium space since the TMDI is fully contained within a single (last) floor which is commonly reserved for accommodating various building services, and (2) top-storey softening can be readily achieved by simple local modifications such as discontinuation of the core at the last floor as well as increasing the top-storey height as depicted in Figure 1(a).

Herein, the effectiveness of top-storey softening to improve TMDI motion control efficiency is numerically illustrated with the aid of a 34-storey composite core-frame building structure shown in Figure 1(b) subject to a parametrically defined stochastic across-wind force model accounting for VS effects. An optimal TMDI design problem is formulated and numerically solved to minimize floor acceleration (i.e., occupants' comfort criterion) of the case-study building in which top-floor height along with TMDI inertial properties (i.e., mass and inertance) are explicitly taken into consideration. Optimal TMDI-equipped structure performance is assessed in terms of floor acceleration, TMDI stroke, and damping and inerter forces and attention is focused to quantify gains in the required attached mass and to check for occupants' comfort criteria. The presentation begins with a brief description of the case-study building and its numerical modelling enabling efficient TMDI incorporation and dynamic analysis.

## 2 CASE-STUDY BUILDING STRUCTURE AND NUMERICAL MODELLING

The adopted structure is 110.6m high and has square 24m-by-24m footprint as shown in Figure 2(b). The lateral load-resisting structural system is composite consisting of a perimeteric three-bay per side steel moment resisting frame (MRF) and a central reinforced concrete (r/c) core. MRF members are rigidly connected and have hollow rectangular sections with varying dimensions along the building height. The r/c core has 8m-by-8m plan-view dimensions and consists of outer wall segments whose thickness reduces progressively with building height and inner (stiffening) wall segments with same thickness along the building height. Hinged primary beams are used to couple the MRF with the core at each floor level which do not participate in resisting lateral loads and floor slabs behave as rigid diaphragms. The total mass of the structure accounting for dead and live loads,  $M_{tot}$ , is 92830tons and is distributed at each floor level as shown in Figure 1(c). To expedite computational work required in TMDI optimal design, a planar dynamic model with 34 degrees of freedom (DOFs) corresponding to the uncoupled lateral in-plane translations of rigid slabs along the across-wind direction of the case-study building is defined in terms of a diagonal mass matrix,  $\mathbf{M}_s \in \mathbb{R}^{34 \times 34}$ , and full stiffness and damping matrices,  $\mathbf{K}_s \in \mathbb{R}^{34 \times 34}$  and  $\mathbf{C}_s \in \mathbb{R}^{34 \times 34}$ , respectively. The main diagonal of the  $\mathbf{M}_s$  matrix is populated with the lumped floor masses of Figure 1(c). Further, the stiffness matrix  $\mathbf{K}_s$  is obtained from a detailed linear finite element (FE) model of the lateral load-resisting structural system of the building developed in SAP2000® software package. The accuracy of the modal properties (mode shapes and natural frequencies) of the 34-DOF dynamic model is verified against modal analysis results from the detailed FE model. Lastly, the inherent structural damping is incorporated in the modelling through a full damping matrix  $\mathbf{C}_s$  obtained by assuming

modal damping ratios  $\zeta_j = 1\%$  for  $j = 2,3,4$ ;  $\zeta_j = 2\%$  for  $j = 5,6,7$ ;  $\zeta_j = 4\%$  for  $j = 8,9,10$ ;  $\zeta_j = 8\%$  for  $j = 11, \dots, 20$ ; and  $\zeta_j = 16\%$  for  $j = 21, \dots, 34$ .

### 3 WIND EXCITATION MODEL

The input wind action to the 34-DOF dynamic model capturing the across-wind dynamics of the case-study building is herein represented by the stochastic across-wind force model developed in [2] for buildings with rectangular footprint. This wind forcing model is based on wind tunnel testing data and accounts for both the turbulence and the VS components of the wind force in the across-wind direction. It is defined by a zero-mean stationary Gaussian spatially correlated random field represented in frequency domain by a full power spectral density (PSD) matrix. For the 34-DOF dynamic model, a  $S_{FF}^{34} \in \mathbb{R}^{34 \times 34}$  wind force PSD matrix is determined upon spatial discretization of the wind random field at each building floor. The assumed mean wind velocity profile is plotted in Figure 2(a). It follows the Eurocode-compliant logarithmic law [18] and terrain category IV (i.e., area in which at least 15% of the surface is covered with buildings and their average height exceeds 15 m) and is defined for basic wind velocity of 22m/s (i.e., 10mins mean wind velocity at 10m height above open flat terrain). For illustration, wind force PSDs computed by the model in [2] at four different floor slab heights are plotted in Figure 2(b) following the assumed mean wind velocity profile.

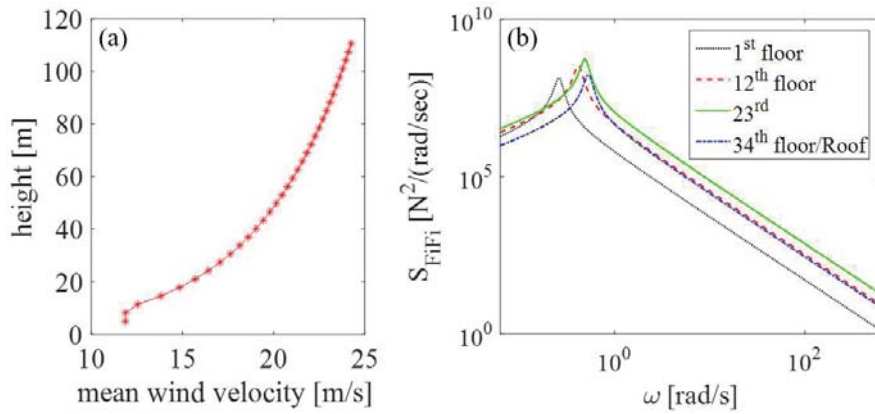


Figure 2. Assumed wind excitation model: (a) mean wind velocity profile, (b) power spectral density functions (PSDs) of across-wind forces acting at different floor levels of the case-study building.

### 4 TMDI-EQUIPPED STRUCTURE AND FREQUENCY DOMAIN ACROSS-WIND RESPONSE ANALYSIS

Mathematically, a top-floor TMDI is added to the 34-DOF system model following [9,10] to yield a 35-DOF augmented model with mass,  $\mathbf{M} \in \mathbb{R}^{35 \times 35}$ , damping,  $\mathbf{C} \in \mathbb{R}^{35 \times 35}$ , and stiffness,  $\mathbf{K} \in \mathbb{R}^{35 \times 35}$ , matrices written as

$$\mathbf{M} = \begin{bmatrix} m_1 & 0 & \dots & \dots & \dots & 0 \\ & m_2 & \dots & \dots & \dots & \vdots \\ & & \ddots & 0 & 0 & 0 \\ & & & m_{33} + b & 0 & -b \\ SYM & & & & m_{34} & 0 \\ & & & & & m_{TMDI} + b \end{bmatrix}, \mathbf{C} = \begin{bmatrix} c_{1,1} & c_{1,2} & \dots & \dots & c_{1,34} & 0 \\ & c_{2,2} & \dots & \dots & \vdots & \vdots \\ & & \ddots & c_{32,33} & c_{32,34} & 0 \\ & & & c_{33,33} & c_{33,34} & 0 \\ SYM & & & & c_{34,34} + c_{TMDI} & -c_{TMDI} \\ & & & & & c_{TMDI} \end{bmatrix}, \quad (1)$$

$$\text{and } \mathbf{K} = \begin{bmatrix} k_{1,1} & k_{1,2} & \cdots & \cdots & k_{1,34} & 0 \\ & k_{2,2} & \cdots & \cdots & \vdots & \vdots \\ & & \ddots & k_{32,33} & k_{32,34} & 0 \\ & & & k_{33,33} & k_{33,34} & 0 \\ & \text{SYM} & & & k_{34,34} + k_{TMDI} & -k_{TMDI} \\ & & & & & k_{TMDI} \end{bmatrix},$$

in which  $m_k = \mathbf{M}_s[k, k]$ ,  $c_{k,l} = \mathbf{C}_s[k, l]$ , and  $k_{k,l} = \mathbf{K}_s[k, l]$  where  $k, l = 1, 2, \dots, 34$  are the elements of the mass, damping, and stiffness matrices of the uncontrolled host structure, respectively, while the 35-th DOF corresponds to the lateral TMDI mass displacement. Further, in the previous expressions,  $m_{TMDI}$  is the TMDI mass attached to the top (34<sup>th</sup>) floor via a spring with  $k_{TMDI}$  stiffness in parallel with a linear dashpot with damping coefficient  $c_{TMDI}$ , and  $b$  is the inertance of the inerter element highlighted in red in Fig. 1(a), connecting the TMDI mass to the penultimate (33<sup>rd</sup>) floor.

Response displacement, velocity, and acceleration PSD matrices of the TMDI-equipped structure subject to the wind force PSD matrix defined in section 3 can be obtained as

$$\mathbf{S}_{\mathbf{x}\mathbf{x}}(\omega) = \mathbf{B}(\omega)^* \mathbf{S}_{\mathbf{F}\mathbf{F}}(\omega) \mathbf{B}(\omega), \quad \mathbf{S}_{\dot{\mathbf{x}}\dot{\mathbf{x}}}(\omega) = \omega^2 \mathbf{S}_{\mathbf{x}\mathbf{x}}(\omega), \quad \text{and} \quad \mathbf{S}_{\ddot{\mathbf{x}}\ddot{\mathbf{x}}}(\omega) = \omega^4 \mathbf{S}_{\mathbf{x}\mathbf{x}}(\omega) \quad (2)$$

respectively. In Eq. (2),  $\mathbf{S}_{\mathbf{F}\mathbf{F}}(\omega) \in \mathbb{R}^{35 \times 35}$  is the wind force PSD matrix  $\mathbf{S}_{\mathbf{F}\mathbf{F}}^{34}$  augmented by a bottom zero row and a right-most zero column corresponding to the TMDI displacement DOF as the TMDI is internally housed and not subjected to any wind load. Further, the “\*” superscript denotes complex matrix conjugation, and the transfer matrix  $\mathbf{B}$  is given as

$$\mathbf{B}(\omega) = [\mathbf{K} - \omega^2 \mathbf{M} + i\omega \mathbf{C}]^{-1} \quad (3)$$

where,  $i = \sqrt{-1}$ , and the “-1” superscript denotes matrix inversion. Next, response displacement, velocity, and acceleration variance of the  $k$ -th floor are obtained as

$$\sigma_{x_k}^2 = \int_0^{\omega_{\max}} S_{xx}[k, k] d\omega, \quad \sigma_{\dot{x}_k}^2 = \int_0^{\omega_{\max}} S_{\dot{x}\dot{x}}[k, k] d\omega, \quad \text{and} \quad \sigma_{\ddot{x}_k}^2 = \int_0^{\omega_{\max}} S_{\ddot{x}\ddot{x}}[k, k] d\omega, \quad (4)$$

respectively, where  $\omega_{\max}$  is a cut-off frequency above which the energy of the underlying processes is negligible. Moreover, the variance of the relative response displacement, velocity, and acceleration between floors/DOFs  $k$  and  $l$  are obtained by

$$\begin{aligned} \sigma_{x_{k,l}}^2 &= \sigma_{x_k}^2 + \sigma_{x_l}^2 - 2 \int_0^{\omega_{\max}} S_{xx}[k, l] d\omega, \\ \sigma_{\dot{x}_{k,l}}^2 &= \sigma_{\dot{x}_k}^2 + \sigma_{\dot{x}_l}^2 - 2 \int_0^{\omega_{\max}} S_{\dot{x}\dot{x}}[k, l] d\omega, \quad \text{and} \\ \sigma_{\ddot{x}_{k,l}}^2 &= \sigma_{\ddot{x}_k}^2 + \sigma_{\ddot{x}_l}^2 - 2 \int_0^{\omega_{\max}} S_{\ddot{x}\ddot{x}}[k, l] d\omega. \end{aligned} \quad (5)$$

Ultimately, peak response quantities are estimated by multiplying the square root of the variances in Eqs. (4) and (5) with the peak factor  $g$  given by the empirical formula [18]

$$g = \sqrt{2 \ln(\eta T_{\text{wind}})} + \frac{0.577}{\sqrt{2 \ln(\eta T_{\text{wind}})}}, \quad (6)$$

where  $\eta=2\pi/\omega_{n(1)}$  and  $T_{wind}$  is the time duration of exposure to the wind action. In the ensuing numerical work,  $T_{wind}$  is taken equal to 3600s (i.e., one hour of stationary wind excitation is assumed).

## 5 OPTIMAL TMDI DESIGN WITH TOP-STOUREY SOFTENING FOR SERVICEABILITY PERFORMANCE

To investigate the potential of top-storey softening in TMDI-equipped buildings for enhanced serviceability performance under wind excitation, the properties of the TMDI in Fig. 1(a) are optimally designed to mitigate floor accelerations in the case-study building subject to the wind forces defined in section 3. To this aim, an optimal TMDI tuning problem is formulated taking as the objective function (OF) to be minimized the peak floor acceleration of the highest occupied of the case-study building (i.e., the 32<sup>nd</sup> floor). That is,

$$OF=g\sigma_{\ddot{x}_{32}}. \quad (7)$$

The problem has 5 design variables (DVs), namely the top-storey height  $H_{top}$ , the mass ratio  $\mu$ , the inertance ratio  $\beta$ , the TMDI frequency ratio  $\nu_{TMDI}$ , and the TMDI damping ratio  $\xi_{TMDI}$ . The last four DVs are defined as

$$\mu = \frac{m_{TMDI}}{M_{tot}}, \quad \beta = \frac{b}{M_{tot}}, \quad \nu_{TMDI} = \frac{\sqrt{\frac{k_{TMDI}}{m_{TMDI} + b}}}{\omega_1} \quad \text{and} \quad \xi_{TMDI} = \frac{c_{TMDI}}{2\sqrt{(m_{TMDI} + b)k_{TMDI}}}, \quad (8)$$

where  $\omega_1$  is the first natural frequency of the uncontrolled structure. Then, optimal primary DVs,  $\nu_{TMDI}$  and  $\xi_{TMDI}$ , are sought that minimize the OF given values of the secondary DVs,  $H_{top}$ ,  $\mu$ , and  $\beta$ . (secondary design parameters). The optimization problem is numerically solved for the case-study structure using a pattern search algorithm [19] with iteratively updated search range of the primary variables hard-coded in MATLAB®.

## 6 PERFORMANCE ASSESSMENT OF OPTIMAL TMDI-EQUIPPED STRUCTURE WITH SOFTENED TOP-STOUREY

In this section, numerical results are furnished to demonstrate the effectiveness of optimally designed TMDI in containing VS induced vibrations in the case-study building exposed to the PSD wind force matrix as top-floor lateral stiffness reduces. To this aim, TMDIs with different inertance ratios ( $\beta = 0\%$  (TMD), 2%, and 10%) are examined for fixed attached mass  $\mu=0.1\%$  while the top-storey of the case-study building is softened laterally by discontinuing the r/c core at the penultimate (33<sup>rd</sup>) storey (see Fig. 1(a)) and by varying its height within  $H_{top} = [4.0, 6.0]$  (m) interval.

Figure 3(a) reports percentage reduction factor (RF) of peak floor acceleration at the 32<sup>nd</sup> floor of optimal TMDI-equipped structure with respect to the uncontrolled case-study building with coreless top-storey for three different inertance ratios as a function of top-storey lateral stiffness. The latter is given as a percentage of the top-storey stiffness of the case-study structure without r/c core at the 33<sup>rd</sup> storey and  $H_{top}=3.2\text{m}$ . It is observed that optimal TMDI capability to suppress floor accelerations increases appreciably and monotonically as the top-storey stiffness reduces for fixed inertance. On the antipode, for the TMD case (i.e., no inerter and  $\beta = 0\%$ ) acceleration RFs remain practically constant with top-storey flexibility. These results reveal that the presence of the inerter enables improved TMDI vibration control potential as top-storey stiffness reduces. This fact is attributed to the coupling of the acceleration of the attached mass to the acceleration of the 33<sup>rd</sup> floor achieved by the inerter mathematically manifested through

the non-diagonal terms in the mass matrix  $\mathbf{M}$  in Eq. (1). And the herein advocated host-structure modification (i.e., top-storey softening) leverages the positive effect of this coupling in reducing floor accelerations below the top-storey. Nevertheless, when no such coupling exists (i.e., conventional TMD case), top-storey flexibility has no effect to the overall motion control level achieved. In this regard, top-storey lateral stiffness becomes a critical TMDI design parameter. Moreover, it is seen that for given  $\beta$  there is a limiting top-storey stiffness reduction defined by the intersection of the TMD RF curves with the TMDI RF curves, above which the TMD outperforms TMDI. This limiting value increases as inertance increases. Thus, top-storey softening reduces demands for large inertance.

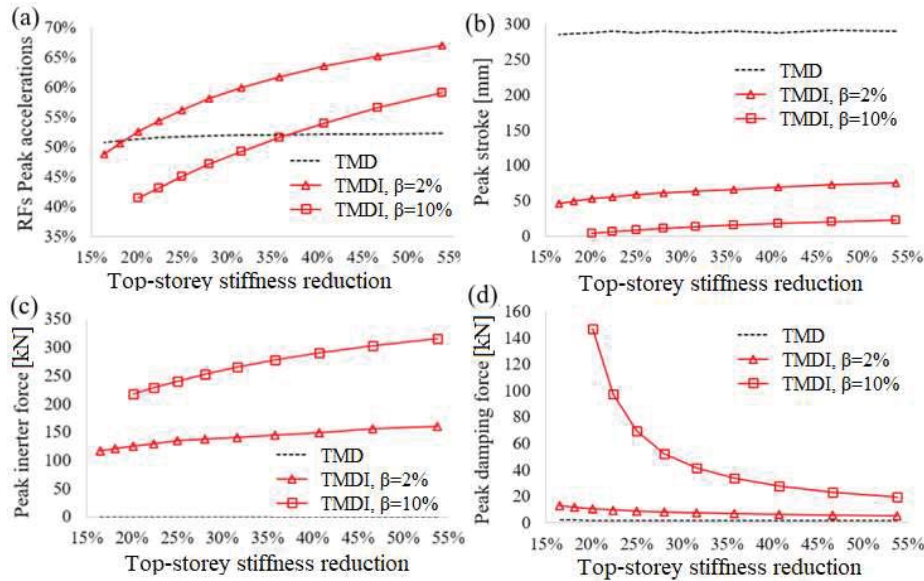


Figure 3. (a) Peak acceleration percentage reduction of 32<sup>nd</sup> floor, (b) secondary mass stroke, (c) peak inerter force, and (d) peak damping force in TMD(I)-equipped structure for attached mass ratio,  $\mu=0.1\%$ , and inertance ratios,  $\beta$ , against lateral top-storey stiffness reduction.

Turning the attention to the peak stroke of the secondary mass, that is, the peak relative displacement of the TMD(I) mass with respect to the floor that the mass is attached to,  $g\sigma_{355,33}$ , Figure 3(b) plots peak TMDI stroke versus top-storey stiffness reduction. It is seen that stroke dramatically reduces with increasing inertance, which is a well-reported effect in the literature [9,10]. Further, stroke demand is positively (though insignificantly) affected by top-storey stiffness reduction. This is quite welcoming result suggesting that the favourable effect of increasing top-storey flexibility to the TMDI effectiveness for suppressing floor accelerations does not come with any increasing cost/demand related to the stroke of the damping device or to the clearance of the secondary mass.

Peak inerter and damping forces developing at the inerter and at the dashpot of optimally designed TMDIs are also deemed essential to check as they need to be economically accommodated locally by the host structure. In this respect, Figures 3(c) and (d) report peak inerter and damping forces, respectively. It is seen that peak inerter force decreases as the top-storey softens at an increasing rate. On the contrary, damping force increases exponentially as the top-storey stiffness reduces for  $\beta = 10\%$ . These trends indicate that top-storey stiffness reduction improves TMDI motion control performance through significant increase of the damping force but not of the inerter force.

Numerical results reported in Figure 3(a) suggest that the same structural performance, in terms of peak floor acceleration, can be achieved by using different sets of secondary design

parameters. From practical viewpoint, this is an important consideration as it enables exchanging attached mass to inertance and/or to top-storey stiffness within a performance-oriented design context. To illustrate this point, Figures 4(a) and (b) plot optimal iso-performance curves on the TMDI inertial  $\mu$ - $\beta$  plane for fixed top-storey stiffness and for fixed performance, respectively. It is seen that all iso-performance curves have negative slope on the  $\mu$ - $\beta$  plane establishing the direct mass reduction/substitution effect endowed by the inertance leading to overall more lightweight inertial dampers. Furthermore, as suggested by Figure 4(b), the same performance can be achieved with reduced average required inertance by approximately 1.6% at  $\mu=0.1\%$ , for every 2% reduction to the top-storey stiffness. As a final remark, top-storey softening further leads to attached mass reduction for fixed inertance to achieve/maintain a preset performance: Figure 4(b) shows that 2% reduction of top-storey stiffness reduces the required mass ratio by about 0.1%, which corresponds to a 20ton TMDI weight reduction for the considered building structure.

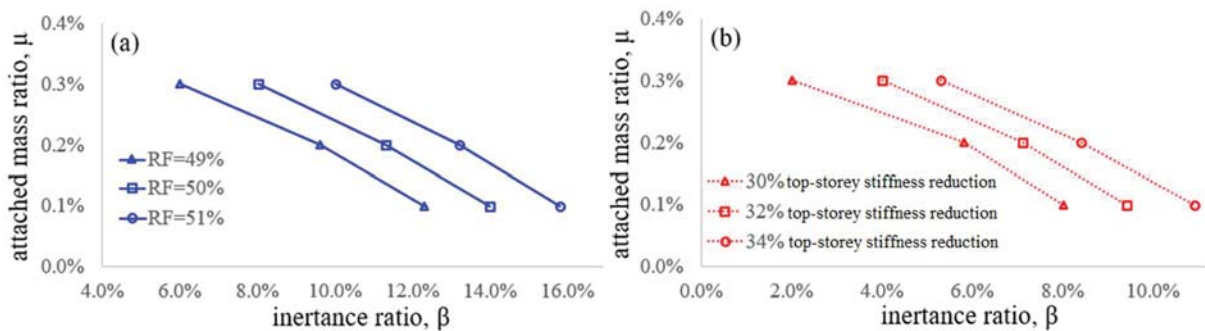


Figure 4. Quantification of mass-inertance-damping coefficient trade-off for (a) fixed normalized stiffness 38%, and (b) fixed performance RF=50%.

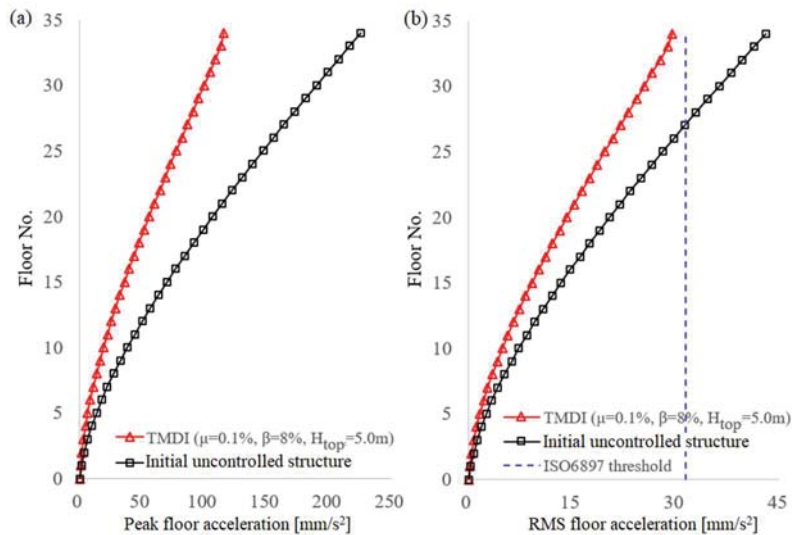


Figure 5. Floor acceleration distribution along the building height and check for occupants' comfort.

As a final check, Figure 5 plots peak and RMS floor accelerations along the building height for the uncontrolled and for a TMDI controlled structure with about 28% top-storey stiffness reduction. The benefit of TMDI is clearly seen and the rationale behind optimal TMDI tuning for minimizing floor acceleration of the 32<sup>nd</sup> floor is justified as it leads to floor acceleration reductions in all lower floors. More importantly, Figure 5(b) shows that the uncontrolled structure did not meet occupants' comfort threshold according to ISO6897 [5] at floors 26 and above

for the specific wind excitation, while the particular optimally tuned TMDI with top-storey softening meets the ISO6897 criterion for all floors.

## 7 CONCLUDING REMARKS

The effectiveness of optimally tuned top-storey TMDIs in conjunction with local top-storey softening has been numerically explored for mitigating floor accelerations in the across-wind direction of slender core-frame buildings which become critical for serviceability design associated with occupants' comfort. Numerical results for different TMDI inertance and top-storey stiffness have shown that improved structural performance in terms of peak floor acceleration and attached mass stroke are achieved by increasing inertance and/or by reducing top-storey stiffness for fixed TMDI attached mass. Meanwhile no improved performance is achieved by conventional TMD through top-storey softening. It was further demonstrated that the required TMDI mass/weight can be reduced either by increasing inertance or by softening the top-storey for a preset performance level. Therefore, top-storey softening facilitates practical implementation of TMDI as it relaxes requirements for large inertance.

## REFERENCES

- [1] A. Kareem, T. Kijewski, Y. Tamura, Mitigation of motions of tall buildings with specific examples of recent applications, *Wind and Structures* 2(3), 201-251, 1999.
- [2] Q.S. Li, L.H. Zhi, A.Y. Tuan, C.S. Kao, Dynamic behavior of Taipei 101 Tower: Field measurement and numerical analysis, *J. Struct. Eng.* 137, 143-155, 2011.
- [3] S. Elias, V. Matsagar, Research developments in vibration control of structures using passive tuned mass dampers, *Annual Reviews in Control* 44, 129-156, 2017.
- [4] S. Liang, S. Liu, Q.S. Li, L. Zhang, M. Gu, Mathematical model of across-wind dynamic loads on rectangular tall buildings. *J. Wind Eng. Ind. Aerodyn.* 90, 201-251, 2002.
- [5] Guidelines for the evaluation of the response of occupants of fixed structures to low frequency horizontal motion (0.063 to 1 Hz), *ISO Standard 6897*, 1984.
- [6] M. Ciampoli, F. Petrini, Performance-Based Aeolian Risk assessment and reduction for tall buildings, *Prob. Eng. Mech.* 28, 75-84, 2012.
- [7] M. De Angelis, S. Perno, A. Reggio, Dynamic response and optimal design of structures with large mass ratio TMD, *Earthquake Eng. Struct. Dyn.* 41, 41-60, 2012.
- [8] K. Tse, K. Kwok, Y. Tamura, Performance and Cost Evaluation of a Smart Tuned Mass Damper for Suppressing Wind-Induced Lateral-Torsional Motion of Tall Structures, *J. Struct. Eng.* 138(4), 514-525, 2012.
- [9] A. Giaralis, F. Petrini, Wind-induced vibration mitigation in tall buildings using the tuned mass damper-inerter (TMDI), *J. Struct. Eng.* 143(9), 04017127, 2017.
- [10] F. Petrini, A. Giaralis, Z. Wang, Optimal tuned mass-damper-inerter (TMDI) design in wind-excited tall buildings for occupants' comfort serviceability performance and energy harvesting, *Eng. Struct.* 204, 109904, 2020.
- [11] M.C. Smith, Synthesis of Mechanical Networks: The Inerter, *IEEE Trans. Automat. Control* 47(10), 1648-1662, 2002.

- [12] L. Marian, A. Giaralis, Optimal design of inerter devices combined with TMDs for vibration control of buildings exposed to stochastic seismic excitations, *Proc. 11th ICOSSAR Int. Conf. on Structural Safety and Reliability*, 1025-1032, 2013.
- [13] L. Marian, A. Giaralis, Optimal design of a novel tuned mass-damper–inerter (TMDI) passive vibration control configuration for stochastically support-excited structural systems, *Prob. Eng. Mech.* 38, 156–164, 2014.
- [14] R. Ruiz, A.A. Taflanidis, A. Giaralis, D. Lopez-Garcia, Risk-informed optimization of the tuned mass-damper-inerter (TMDI) for the seismic protection of multi-storey building structures, *Eng. Struct.* 177, 836-850, 2018.
- [15] S. Nakaminami, H. Kida, K. Ikago, N. Inoue, Dynamic testing of a full-scale hydraulic inerter-damper for the seismic protection of civil structures, *7th International conference on advances in experimental structural engineering*, 41-54, 2016.
- [16] D. Pietrosanti, M. De Angelis, A. Giaralis, Experimental study and numerical modeling of nonlinear dynamic response of SDOF system equipped with tuned mass damper inerter (TMDI) tested on shaking table under harmonic excitation, *Int. J. Mech. Sci.* 184(15), 105762, 2020.
- [17] S.B. Taranath, *Tall Building Design, Steel, Concrete, and Composite Systems*. ISBN: 9781466556201, 2017.
- [18] A.G. Davenport, Note on the distribution of the largest value of a random function with application to gust loading, *Proc. of the Institution of Civil Engineers* 28(2), 187-196, 1964.
- [19] A. Charles, J.E. Dennis, Analysis of Generalized Pattern Searches, *SIAM Journal on Optimization* 13(3), 889–903, 2003.